PROCEEDINGS OF THE ROYAL SOCIETY B

rspb.royalsocietypublishing.org

Research

Cite this article: Murdock DJE, Sansom IJ, Donoghue PCJ. 2013 Cutting the first 'teeth': a new approach to functional analysis of conodont elements. Proc R Soc B 280: 20131524. http://dx.doi.org/10.1098/rspb.2013.1524

Received: 12 June 2013
Accepted: 22 July 2013

Subject Areas:
palaeontology

Keywords:
vertebrata, Conodonta, *Panderodus*, function, second moment of inertia

Authors for correspondence:
Duncan J. E. Murdock
e-mail: duncan.murdock@bristol.ac.uk
Philip C. J. Donoghue
e-mail: phil.donoghue@bristol.ac.uk

Electronic supplementary material is available at http://dx.doi.org/10.1098/rspb.2013.1524 or via http://rspb.royalsocietypublishing.org.

Royal Society Publishing
Informing the science of the future

Cutting the first 'teeth': a new approach to functional analysis of conodont elements

Duncan J. E. Murdock[1], Ivan J. Sansom[2] and Philip C. J. Donoghue[1]

[1]School of Earth Sciences, University of Bristol, Wills Memorial Building, Queen's Road, Bristol BS8 1RJ, UK
[2]School of Geography, Earth and Environmental Sciences, University of Birmingham, Birmingham B15 2TT, UK

The morphological disparity of conodont elements rivals the dentition of all other vertebrates, yet relatively little is known about their functional diversity. Nevertheless, conodonts are an invaluable resource for testing the generality of functional principles derived from vertebrate teeth, and for exploring convergence in a range of food-processing structures. In a few derived conodont taxa, occlusal patterns have been used to derive functional models. However, conodont elements commonly and primitively exhibit comparatively simple coniform morphologies, functional analysis of which has not progressed much beyond speculation based on analogy. We have generated high-resolution tomographic data for each morphotype of the coniform conodont *Panderodus acostatus*. Using virtual cross sections, it has been possible to characterize changes in physical properties associated with individual element morphology. Subtle changes in cross-sectional profile have profound implications for the functional performance of individual elements and the apparatus as a whole. This study has implications beyond the ecology of a single conodont taxon. It provides a basis for reinterpreting coniform conodont taxonomy (which is based heavily on cross-sectional profiles), in terms of functional performance and ecology, shedding new light on the conodont fossil record. This technique can also be applied to more derived conodont morphologies, as well as analogous dentitions in other vertebrates and invertebrates.

1. Introduction

Conodonts are an extinct group of primitive jawless vertebrates [1] that bore phosphatic tooth-like elements, with a diversity of form comparable with the dentition of all other vertebrates [2]. These elements formed an oropharyngeal feeding array at the anterior of an eel-like animal, and were used to capture and process prey. Despite being the earliest vertebrates with mineralized tissues [3,4], and a notable component of marine ecosystems from the Cambrian to the Triassic [5], the range in feeding ecology of this group is virtually unknown. In the 'complex' conodonts (prioniodontids, *sensu* [5]), the apparatus can be divided broadly into two suites of morphologically distinct elements: an array of rostral food acquisition ramiform elements (bearing a number of more or less elongate processes); and pairs of caudal 'platform' (blade-like and molar-like) elements proposed to perform a role in food processing [6]. Functional interpretations of conodont elements, beyond gross assignments to broad ecotypes such as 'grasping' or 'slicing', have been limited to platform elements in these extremely derived conodonts [7–12]. Functional analysis of coniform conodont elements, which are a significant component of conodont diversity from the Late Cambrian through to the Devonian and also reflect the plesiomorphic morphology, is hampered by a lack of clarity over how to explore their functional morphology, except by comparison with dentitions of similar morphology in other vertebrates [13]. Most functional analyses of 'complex' conodonts rely on modelling occlusion of platform elements [2,10], but these are inappropriate for coniform elements. An alternative approach is to estimate the inherent mechanical properties of the elements from their morphology. Coniform conodont elements can be treated as beams, anchored at the base (i.e. a cantilever) and loaded at the tip of the cusp in one direction during feeding. Two important features of a loaded beam are resistance to bending (second moment of area, I) and resistance to torsion (polar moment of area, J). Both of these give an indication of how the beam/element will respond to forces exerted

by prey items during feeding, and both can be estimated by examining the cross-sectional profile of the element.

Here, we estimate the properties of coniform elements from their cross-sectional profile, an approach proven in the assessment of the mechanical properties of a range of structures in vertebrates [14,15], but never before applied to conodont elements. Although coniform conodont elements are widely considered to have performed a grasping function, there is evidence of morphological and, therefore, inferred functional differentiation within most apparatuses [16]. Second moment of area represents an appropriate analytical test of these hypotheses, because it measures bending resistance, which is the principal property of grasping elements.

2. Material and methods

Our study is based on *Panderodus* (Vertebrata, Conodonta, Panderodontida, Panderodontidae), a genus bearing coniform elements that was common and widespread in the Ordovician and Silurian. *Panderodus* elements can be described broadly as recurved, laterally furrowed cones, and are known to have been organized into apparatuses of 17 elements, encompassing six distinct morphotypes, and interpreted to have been arranged in three architectural units (figure 1). The apparatus reconstruction for *Panderodus* is based on the analysis of both large collections of discrete isolated elements that have been studied extensively, as well as fused clusters of multiple elements from a single individual, preserving some of the original relative disposition of the elements [16]. The confidence with which this apparatus has been reconstructed, and the relatively simple yet clearly differentiated element morphology makes *Panderodus* an ideal model in which to investigate the functional morphology of coniform conodonts. Its differentiated apparatus allows us to explore the hypothesis of differentiated function, but variance in morphology among elements within the apparatus serves as a proxy for investigating the functional significance of coniform element morphology more generally.

Following the apparatus reconstruction of Sansom *et al.* [16], six element morphotypes of *Panderodus acostatus*, from a single sample of the Upper Visby beds, basal Wenlock, Gotland, Sweden, were characterized volumetrically using synchrotron radiation X-ray tomographic microscopy (SRXTM) [18]. From this tomographic dataset, three-dimensional renderings of the external morphology of each element were made, and virtual sections derived.

For the functional analysis (see electronic supplementary material and figure 1), virtual sections were taken through each element orthogonal to the midline of the specimen, at approximately 25%, 50% and 75% along the length of the element from the proximal end of the crown to the tip of the cusp, and converted into solid silhouettes depicting element cross-sectional shape. These silhouettes were read into ImageJ and processed using the MomentMacroJ plug-in, to estimate the second moment of area (resistance to bending) and polar moment of area (resistance to torsion) of each element.

Moment of area is directly related to how material is distributed with regard to a given axis (the neutral bending axis); second moment of area (I) for an axis in the plane, polar moment of area (J) for an axis perpendicular to the plane. Second moment of area for a filled ellipse, with major and minor axes a and b, is calculated thus: $I_0 = (\pi.ab^3)/4$; therefore, the value of I for a given axis has an exponential relationship to the relative length of that axis, and values of I for any axis of a circle will be the same. Polar moment of area is calculated by summing the I for the axes with the maximum and minimum values and, thus, takes into account the overall shape. The distribution of material in a given axis during loading is related directly to the degree to which the beam will be deflected. In this case, we are interested in how much the elements will resist bending (second moment of area), to facilitate penetration of a prey item, and how much the elements will resist torsion (polar moment of area) to maintain the prey item in a given (favourable) position.

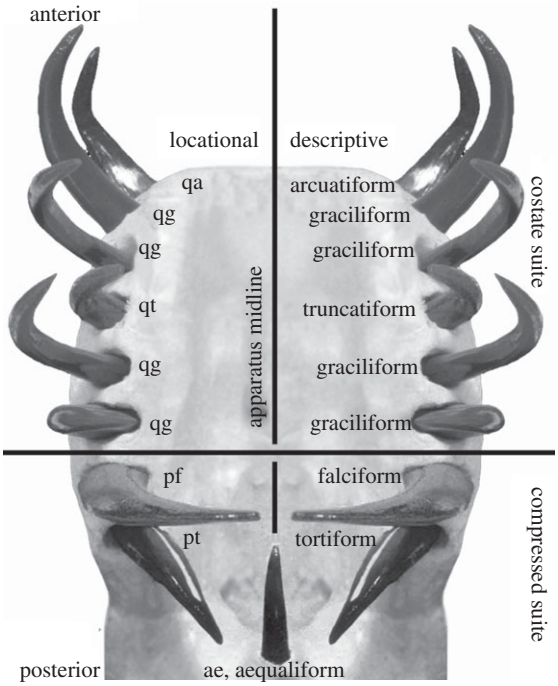

Figure 1. Architectural reconstruction of the *Panderodus* apparatus. Physical model photographed in ventral view. Six morphotypes are included in the apparatus, eight pairs of recurved elements and one unpaired element symmetrical about the midline. There are four pairs of graciliform elements; asymmetric high- and low-based forms and subsymmetric high- and low-based forms. Note the anterior–posterior differentiation of the paired elements into two morphologically (and, by inference functionally) distinct suites. The aequaliform element is thought to have lain near the midline near the posterior of the apparatus. Reconstruction based on Sansom *et al.* [16] and Smith *et al.* [17].

As the elements used were isolated specimens from an assemblage of disarticulated skeletons, the results of these calculations were scaled based on natural articulated assemblages known to represent elements from single individuals (in particular, using the Waukesha [17] and Nekézseny [19,20] natural assemblages both illustrated in Sansom *et al.* [16]) to reflect the relative size of elements *in vivo*. To exploit the natural variation in the elements comprising the *Panderodus* apparatus as a proxy for variation in coniform element morphology more generally, the virtual sections were rescaled by dividing by the square of their cross-sectional area. This allows for the comparison of shape only, and the effect of individual morphological features can be assessed. Our analyses focused on the enamel-like tissues that comprise the crown of the elements. The effect of including the dentine-like 'basal body', and basal cavity was tested by digitally filling in the cavity for the cross section with the largest hollow proportion (arcuatiform element; 9.1% hollow at the one-fourth cross section) and repeating the moment calculations. The values for I increased by less than 2%, i.e. within the error of the calculations. In addition, the low inferred Young's modulus for the basal body means it would contribute relatively little to the value of I compared with an element formed totally of crown tissue. Therefore, the presence of the basal cavity can be ignored.

In order to further investigate the effect of cross-sectional profile on resistance to bending, a series of artificial cross sections were characterized. Each of the six shapes (a simple ellipse, and five shapes reflective of the range of conodont element cusp morphologies) were compared across the same range of aspect ratios and scaled to the same cross-sectional area.

In all instances, we have considered the mechanical properties of the elements *in vacuo*, because the nature of the attachment of conodont elements to the surrounding soft tissue is entirely unknown.

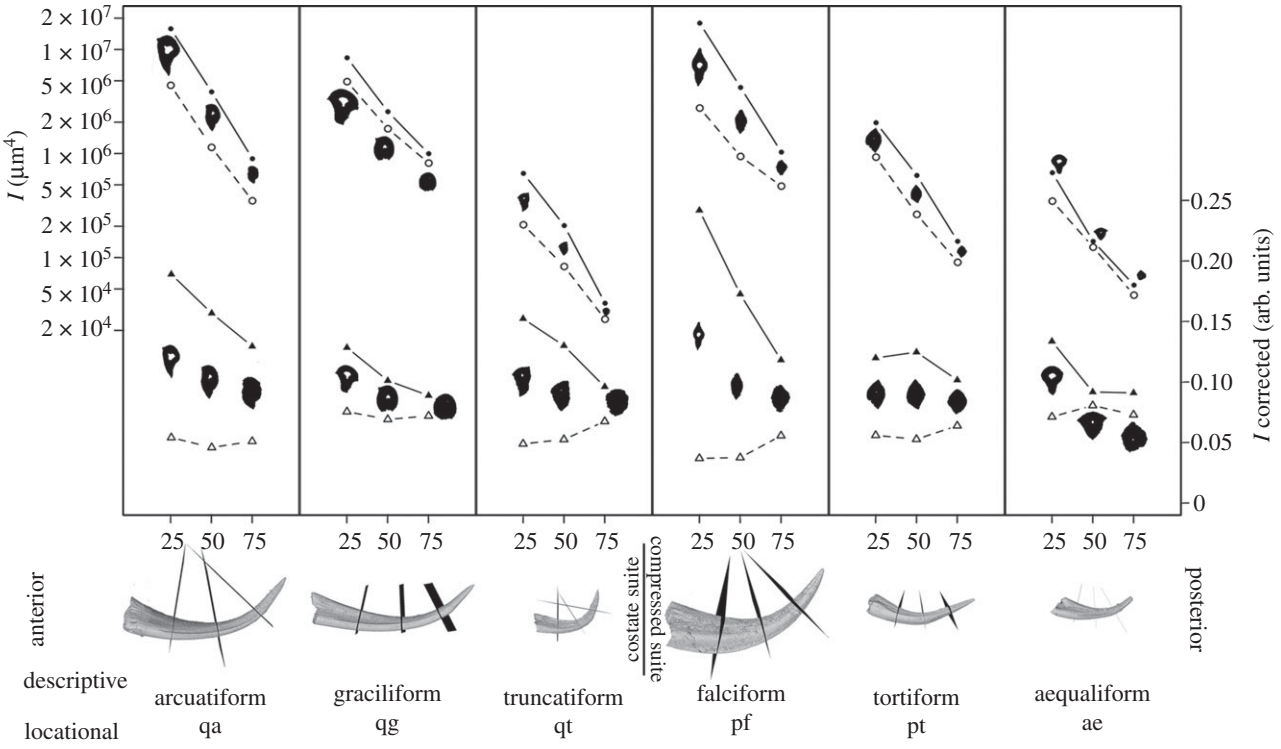

Figure 2. Variation in second moment of inertia across the *Panderodus* apparatus, and within individual elements. Maximum (solid lines) and minimum (dashed lines) estimates shown for each element for sections along the element from proximal to distal. Circles, and left-hand axis, elements scaled to *Panderodus* apparatus. Triangles, and right-hand axis, size-detrended data (sections are of equal area). Elements are arranged from anterior (left) to posterior (right), SRXTM surface renderings with position and orientation of sections for reference, silhouettes of cross section shown for reference, reoriented with axis of greatest resistance to bending as vertical.

3. Results

(a) Estimating second moment of inertia

In the uncorrected data (figure 2, circles), size (cross-sectional area) positively correlates strongly with both maximum and minimum second moment of area. This is to be expected given area is effectively part of the moment calculation. After removing area by dividing by area squared (figure 2, triangles) the aspect ratio of the cross sections has the greatest effect on resistance to bending. Cross sections tending towards a circle (e.g. those of the graciliform element) have similar values for I in both x- and the y-directions (each element tends towards a circular cross section distally, proximal to the tip). Increasingly elliptical cross sections (e.g. those of the falciform element) have much higher values of I for loads applied along the long axis, and correspondingly smaller values in the short axis. In addition, cross-sectional profiles closer to being circular (e.g. the aequaliform element) have close to uniform second moment of inertia in all orientations, and the assignment of 'major' and 'minor' axes becomes somewhat arbitrary.

(b) Polar moment of area estimations

Polar moment of area (the sum of moments of inertia about axes at right angles to each other) is a measure of resistance to torsion. In the uncorrected data, the size difference between elements dominates the values for polar moment of area, with the larger elements being more resistant to torsion. However, when size differences are removed, the data reveal a more subtle pattern, dictated by shape. The aequaliform and truncatiform elements are symmetrical and relatively equant in cross section, and so then have relatively higher resistance to torsion when compared with the pattern when size differences are included. Conversely, the graciliform and tortiform elements show the opposite pattern (table 1).

Table 1. Summary of results of polar moment of area calculations ranked from most resistant (1) to least resistant to torsion (6). Units arbitrary for size-removed data.

rank	element; polar moment (μM^4)	element; size-detrended polar moment
1	pf; 2.07×10^7	pf; 2.79×10^{-1}
2	qa; 2.03×10^7	qa; 2.43×10^{-1}
3	qg; 1.32×10^7	ae; 2.05×10^{-1}
4	pt; 2.90×10^6	qg; 2.04×10^{-1}
5	ae; 1.00×10^6	qt; 2.01×10^{-1}
6	qt; 8.51×10^5	pt; 1.76×10^{-1}

(c) Artificial cross sections

Size and aspect ratio do not explain all of the variance shown in resistance to bending. Comparing the size-removed data for each element with predicted values for an ellipse of comparable aspect ratio, many of the element cross sections have considerably higher maximum resistance to bending, yet broadly comparable minimum values (figure 3*a*). Thus, morphological specialization correlates to an improved resistance to bending. The results from analysis of the artificial cross sections show a broadly similar pattern; three morphotypes (figure 3*b–d*) show successively higher maximum values of I, with comparable minimum values. The fourth morphotype (figure 3*e*) shows the highest maximum values, but with a corresponding reduction in minimum values. Finally, the cruciform cross section (figure 3*f*) has the same pattern of results for second moment of area as an ellipse, but with all values displaced positively.

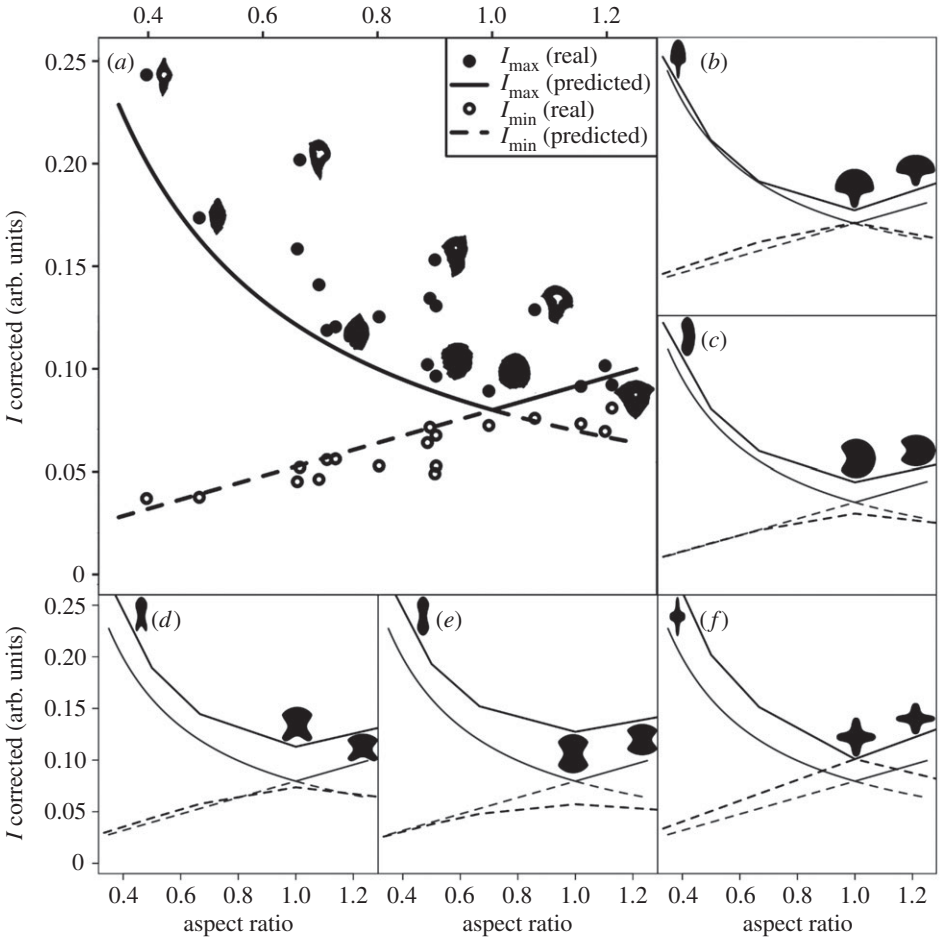

Figure 3. Comparison of second moment of inertia between *Panderodus* elements and artificial cross sections. Maximum (solid lines) and minimum (dashed lines) estimates shown for each element for sections plotted against aspect ratio (*x*/*y*). (*a*) Comparison of real maximum (solid circles) and minimum (open circles) values of *Panderodus* elements with those predicted for an eclipse with a range of aspect ratios. Some representative silhouettes of *Panderodus* cross sections for reference. (*b*–*f*) Comparison of predicted value for an ellipse (grey) with those for five artificial cross sections (black), shape of cross section at maximum, minimum and 1 : 1 aspect ratio shown with orientation of I_{max} vertical and I_{min} horizontal shown in each plot. (*b*–*f*) All plotted on the same axes.

4. Discussion

(a) Differentiation of function within the *Panderodus* apparatus

Morphological variation between elements of *Panderodus* suggests functional specialization between different parts of the apparatus (figure 4). The largest elements, and therefore those elements most resistant to bending and torsion, are generally found at the anterior of the apparatus. This pattern is reinforced by the repetition of graciliform elements in individual animals, indicating the anterior of the apparatus would be subject to the greatest bending forces, such as encountered in prey capture. The graciliform elements also display the smallest difference in resistance to bending in the maximum and minimum direction, suggesting they were best adapted to restraint of prey (which would apply loads in multiple directions). In addition, the graciliform and arcuatiform elements have the greatest resistance to torsion (excepting the falciform element), ideally suited to prey restraint at the anterior of the apparatus.

In addition, there is differentiation within the apparatus in terms of both shape and relative abundance of crown, basal body and basal cavity [16]. Arcuatiform, truncatiform and especially falciform, elements are considerably stiffer in one plane than the other. This would be of the greatest utility if they experienced loading in one orientation, functioning like a blade, suggesting they are likely to perform comparatively better in cutting prey items. In addition, these element morphotypes have larger crowns, relative to their basal body, than comparably sized elements of other morphologies. Taking into consideration the fact that bending stiffness of the elements would have been a function of both the polar moment (I) and Young's modulus (E) of the material (considerably higher in crown tissue than the basal body, discussed in Jones *et al.* [2]), the histological data also support the interpretation of these elements as having performed a role in piercing or cutting prey, with a much greater bending stiffness ($=EI$) in one plane than the other. By contrast, graciliform, tortiform and aequaliform elements are more equally resistant to bending in both directions, and have proportionally smaller crowns, and so would have had a much more evenly distributed bending resistance, seemingly adapted for prey capture and restraint.

The previously erected division of the apparatus into three architectural units (paired costate (anterior) and compressed (posterior) suites, and a medial unpaired aequaliform element) [16] does not translate readily into functional differentiation as subtle differences appear within each of these divisions. The apparatus superficially displays (figure 2, circles) a repeated pattern of decreased resistance to bending posteriorly (qa > qg > qt and pf > pt > ae). This is not an altogether fair representation of the co-state suite because it does not take into account the repetition of pairs of graciliform elements (qa > qg = qg > qt < qg = qg). In addition, the aequaliform

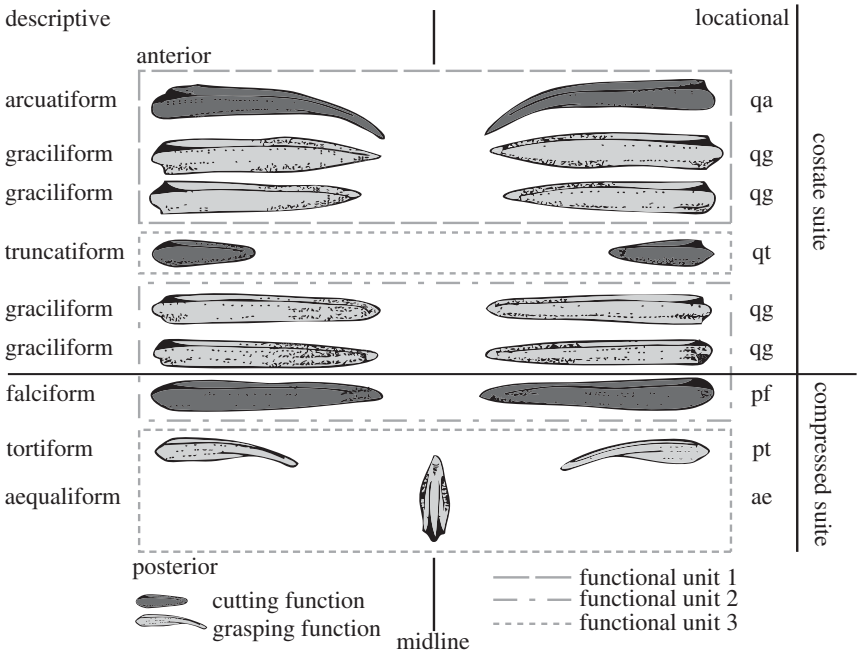

Figure 4. New functional hypothesis mapped onto the architectural reconstruction of the *Panderodus* apparatus. Element shading represents proposed function of each element based on the calculated moments of area. Elements are grouped into functional units and boxed (each containing a pair of 'cutting' elements) based on likely timing of contact between cusps and prey items. Adapted from Sansom *et al*. [16].

element is oriented perpendicular to the paired elements. This suggests a threefold architectural division is an over simplification of element function within the apparatus.

Based on the relative size and positions of the elements within the apparatus reconstruction, with large arcuatiform and graciliform elements at the anterior and smaller tortiform and aequaliform elements at the posterior (figure 1), it is possible to group elements based on their likely relative timing of contact of their cusps with prey items. Three potentially, distinct functional units can be identified (figure 4), each containing 'cutting' and 'grasping' elements: an anterior unit consisting of arcuatiform and graciliform elements; a posterior unit consisting of falciform and graciliform elements; and the smaller truncatiform, tortiform and aequaliform elements forming a third unit. This interpretation is also supported by the polar moment of area estimations, where the third unit is comprised of elements with the lowest resistance to torsion and is consistent with these being the final elements to make contact with prey items, i.e. not involved in prey restraint.

(b) Available cross sections and implications for other coniform taxa

Panderodus is one of the few coniform conodont taxa for which data are available on elements' relative size within the apparatus. Inferences of function for the remainder of taxa must therefore be based on shape differences. Thus, in attempting to use shape variation within the apparatus of *Panderodus* as a proxy for shape variance more generally, we normalized the size of the elements so that we could examine the effects of element shape *in vacuo*.

Firstly, after removing area, aspect ratio emerges as the largest component for determining resistance to bending. Cross sections more closely resembling a circle will have similar resistance to bending in both x- and y-directions. This is clear from the convergence of maximum and minimum values as each element tends towards a circle in cross section proximal to the tip, to varying degrees. By contrast, higher values of I in the long axis compared with the short axis are characteristic of broadly elliptical cross sections. However, the maximum resistance to bending exhibited by the size-removed cross sections is consistently greater than that expected from an ellipse of equivalent aspect ratio (figure 3*a*). A qualitative analysis of the cross-sectional profiles in comparison with the ellipse model prediction (representatives shown in figure 3*a*) demonstrated that concentrating material along the axis in line with loading improves the resistance to bending in that axis. This interpretation is supported by our analysis of artificial cross sections, where the cross sections have only one axis of symmetry (figure 4*b–d*), the maximum values of I are higher than those predicted by an ellipse, whereas the minimum values are comparable.

The two remaining morphotypes (figure 4*e,f*) serve to explain a second significant factor that is commonly used in the construction of loaded beams. When bending, the upper and lower surfaces are in tension and compression, respectively, whereas the centre of the beam does not undergo deformation. Thus, removing material from the centre of the beam does not reduce its ability to resist bending (as in a hollow tube), but concentrating material along one axis increases resistance to bending in that axis. These factors are reflected in the prevalence of 'I' beams in construction. The fourth morphotype (figure 3*d*) approximates an 'I' shape, with reduction of material in the centre and along one axis, with a corresponding increase in maximum second moment of area. However, as with 'I' beams, there is a corresponding reduction in minimum values. Two planes of symmetry reduce the contrast between maximum and minimum values of I. Indeed, they converge on the same value in shapes with fourfold or radial symmetry, such as a circle or the fifth morphotype (figure 3*f*). This cruciform cross section combines both the advantage of reducing mass in areas under less stress, but not in just one orientation. The *Panderodus* cross sections with the highest aspect ratio, which might be expected to have very low second moment of area in the horizontal axis, resemble this cruciform cross section, reducing the effect of a high aspect ratio. For a given amount of material, a hollow tube will have an increased resistance to bending than a solid rod (although a much larger diameter). In addition to the comparatively stiff enamel-like

tissues of the element crown that surrounds the dentine-like basal body, many coniform conodonts have a basal cavity extending part of the way through the element, making them effectively hollow, at least in part. This reflects the mode of growth of the elements, but may also reflect an adaptation to increase bending resistance. However, in the cross section with the largest basal cavity (arcuatiform element at one-fourth along the length), only 9.1% of the total area is hollow. If the basal cavity is infilled artificially with crown tissue, a small increase in bending resistance is observed (less than 2%), but it is orders of magnitude smaller than the effect of changing aspect ratio or morphology, and within the error of the calculations. The lack of a straw-like morphology (i.e. very large central cavity and thin walls) in conodonts may reflect the need to maintain a relatively small basal cavity (and therefore thickness of the element walls) to resist deformation during compression orthogonal to the long axis of the elements.

The results of this analysis have impact beyond the function of the *Panderodus* apparatus. Panderodontids are extreme amongst coniform conodonts in terms of their apparatus differentiation. Non-panderodontid taxa, such as *Besselodus* [21], *Parapanderodus* [22] and *Drepanodus* [23], have either lower morphological differentiation (i.e. fewer than six morphotypes) within their apparatuses or the majority of the paired elements comprise a morphological continuum (i.e. no distinct morphotypes). This implies a concomitantly lower functional differentiation within the apparatuses of these taxa. In order to test this, the same methodology could be applied to these other coniform conodont elements, and could be used as a proxy for establishing ecological diversity across taxa.

5. Conclusion

The anterior–posterior differentiation of the *Panderodus* apparatus into three architectural suites is not wholly supported by our analysis. Rather, we suggest that there is evidence of morphological and, consequently, functional specialization of individual elements. The evident functional differentiation of the apparatus likely reflects a role in the processing or manipulation, not merely grasping, of food items.

Our study has implications beyond the ecology of a single conodont taxon. Given that taxonomic descriptions of many coniform conodonts rest heavily on cross-sectional profiles, we present a means of examining structural implications of such morphological differences and hence exploring the detailed function(s) of the earliest mineralized vertebrate feeding apparatuses. This provides a basis for reinterpreting coniform conodont evolution, in terms of functional performance and ecology, deriving functional hypotheses that can be tested, for instance, through microwear analysis [9]. The approach that we have exploited can be applied just as readily to the cusps and denticles of more derived conodonts and, indeed, to analogous feeding structures encountered in other vertebrates and invertebrates [13].

Acknowledgements. We thank Colin Palmer, Phil Anderson, Paul Smith and Emily Rayfield for invaluable discussion, and the insightful comments of two anonymous referees which greatly improved the manuscript. Simon Powell assisted in the making of the figures.

Funding statement. This work was funded by NERC Studentship to D.J.E.M.

References

1. Aldridge RJ, Briggs DEG, Smith MP, Clarkson ENK, Clark NDL. 1993 The anatomy of conodonts. *Phil. Trans. R. Soc. Lond. B* **340**, 405–421. (doi:10.1098/rstb.1993.0082)
2. Jones D, Evans AR, Siu KKW, Rayfield EJ, Donoghue PCJ. 2012 The sharpest tools in the box? Quantitative analysis of conodont element functional morphology. *Proc. R. Soc. B* **279**, 2849–2854. (doi:10.1098/rspb.2012.0147)
3. Sansom IJ, Smith MP, Armstrong HA, Smith MM. 1992 Presence of the earliest vertebrate hard tissues in conodonts. *Science* **256**, 1308–1311. (doi:10.1126/science.1598573)
4. Donoghue PCJ. 1998 Growth and patterning in the conodont skeleton. *Phil. Trans. R. Soc. Lond. B* **353**, 633–666. (doi:10.1098/rstb.1998.0231)
5. Sweet WC. 1985 Conodonts: those fascinating little whatzits. *J. Paleontol.* **59**, 485–494.
6. Donoghue PCJ, Purnell MA, Aldridge RJ, Zhang S. 2008 The interrelationships of 'complex' conodonts (Vertebrata). *J. Syst. Palaeontol.* **6**, 119–153. (doi:10.1017/s1477201907002234)
7. Purnell MA, Donoghue PCJ. 1997 Architecture and functional morphology of the skeletal apparatus of ozarkodinid conodonts. *Phil. Trans. R. Soc. Lond. B* **352**, 1545–1564. (doi:10.1098/rstb.1997.0141)
8. Nicoll R. 1987 Form and function of the Pa element in the conodont animal. In *Palaeobiology of conodonts* (ed. RJ Aldridge), pp. 77–90. Chichester, UK: Ellis Horwood.
9. Purnell MA. 1995 Microwear on conodont elements and macrophagy in the first vertebrates. *Nature* **374**, 798–800. (doi:10.1038/374798a0).
10. Donoghue PCJ, Purnell MA. 1999 Growth, function, and the conodont fossil record. *Geology* **27**, 251–254. (doi:10.1130/0091-7613(1999)027<0251:GFATCF>2.3.CO;2)
11. Donoghue PCJ, Purnell MA. 1999 Mammal-like occlusion in conodonts. *Paleobiology* **25**, 58–74.
12. Donoghue PCJ. 2001 Microstructural variation in conodont enamel is a functional adaptation. *Proc. R. Soc. Lond. B* **268**, 1691–1698. (doi:10.1098/rspb.2001.1728)
13. Jeppsson L. 1979 Conodont element function. *Lethaia* **12**, 153–170. (doi:10.1111/j.1502-3931.1979.tb00994.x)
14. Jungers WL, Minns RJ. 1979 Computed tomography and biomechanical analysis of fossil long bones. *Am. J. Phys. Anthropol.* **50**, 285–290. (doi:10.1002/ajpa.1330500219)
15. Summers AP, Ketcham RA, Rowe T. 2004 Structure and function of the horn shark (*Heterodontus francisci*) cranium through ontogeny: development of a hard prey specialist. *J. Morphol.* **260**, 1–12. (doi:10.1002/jmor.10141)
16. Sansom IJ, Armstrong HA, Smith MP. 1994 The apparatus architecture of *Panderodus* and its implications for coniform conodont classification. *Palaeontology* **37**, 781–799.
17. Smith MP, Briggs DEG, Aldridge RJ. 1987 A conodont animal from the Lower Silurian of Wisconsin, USA, and the apparatus architecture of panderodontid conodonts. In *Palaeobiology of conodonts* (British Micropalaeontological Society series) (ed. RJ Aldridge), pp. 91–104. Chichester, UK: Ellis Horwood.
18. Donoghue PCJ *et al*. 2006 Synchrotron X-ray tomographic microscopy of fossil embryos. *Nature* **442**, 680–683. (doi:10.1038/nature04890)
19. Kozur H. 1984 Preliminary report about the Silurian to Middle Devonian sequences near Nekézseny (southernmost Uppony Mts., northern Hungary). *Geologische und Palaontologische Mitteilungen, Innsbruck* **137**, 149–176.
20. Balogh K, Kozur H. 1985 The Silurian and Devonian in the surroundings of Nekézseny (southernmost Uppony Mts., northern Hungary). *Acta Mineral. Petrograph. Szeged* **27**, 193–212.
21. Aldridge RJ. 1982 A fused cluster of coniform conodont elements from the Late Ordovician of Washington Land, Western North Greenland. *Palaeontology* **25**, 425–430.
22. Smith MP. 1991 Early Ordovician conodonts of East and North Greenland. *Meddelelser om Grønland, Geosci.* **26**, 1–81.
23. Lofgren AM, Tolmacheva TJ. 2003 Taxonomy and distribution of the Ordovician conodont *Drepanodus arcuatus* Pander, 1856, and related species. *Palaeontol. Zeits* **77**, 203–221.